Published by :
https://www.ijert.org/
An International Peer-Reviewed Journal

International Journal of Engineering Research & Technology (IJERT)
ISSN: 2278-0181
Vol. 14, Issue 09, RTMSE-2026

Performance Evaluation of Nano-coated Balls Being Used in Rzeppa Constant Velocity Joint by using MCDM

Arshpreet Kaur[1, *]

[1]Department of Mechanical Engineering, Punjabi University, Patiala, India;

Jasminder Singh Dureja[1]

Department of Mechanical Engineering, Punjabi University, Patiala, India;

Jasmaninder Singh Grewal[2]

[2]Department of Mechanical and Production Engineering, Guru Nanak Dev Engineering College, Ludhiana, 141006, Punjab, India

[*]Corresponding: arshpandher89@gmail.com

Abstract— ***Rzeppa constant velocity joint plays an important role in the automotive industry because of its primary function to transmit power from the prime-mover to the front wheel-axle. The main element that helps in the smooth movement of the joint are balls that are enclosed inside a cage-like assembly. These balls deteriorate after their continuous use and to avoid these protective coatings are implanted on the surface of balls. The coatings used in this analysis are Latuma and Alcrona Pro deposited on the substrate (EN-19) with the help of PVD-DC Magnetron Sputtering technique. The setup used to investigate the tribological performance in this work is a ball-on-disk apparatus based on the ASTM G-133 standard. The four different experimental conditions explored are with and without lubrication at room temperature as well as at high temperature. To select the best optimum working condition of a rzeppa joint an operation research-based multi-criteria decision-making tool is utilized. The Weightage importance is calculated with the help of entropy weight method and four different ranking techniques utilized are VIKOR, TOPSIS, EDAS, and PROMETHEE-II. Latuma with lubrication at room temperature ranked one in three out of four ranking techniques used in this work.***

Keywords— Nanocoatings, Tribology, Rzeppa joint, MCDM.

1. Introduction

Bearings are important components in different mechanical systems that provide support and reduce friction and wear between two mating parts [1]. Furthermore, it acts as a supporting element for various machine components such as in the case of automobiles in axles, wheels, and various constant velocity joints like rzeppa joint, etc. The elements that act as rotating elements are balls, cylindrical, or taper rollers [2]. It can find a wide range of applications in various fields such as aero-engines, automobiles, high-speed precision spindles, turbine gearboxes, etc. [1]. The Rzeppa constant velocity joint (CVJ) is a homokinetic ball-type joint widely used in automotive drive- train applications that are used for steering movements**.** Different components of the Rzeppa joint are inner rings, outer rings, balls, and boots [3]. In which inner rings are connected to the shaft, the outer rings act as housings as well and balls are placed in between the outer and inner rings in the cage and rubber boots help to protect the joint from failure and increase the life of the joint [4]. There are many reasons for the failure of bearings and damage to the Rzeppa joint such as cracks and fractures due to bearing overloading because of sudden shock loads, and failures because of cavities, and cuts in the track due to entering of foreign elements inside the joint that leads to surface fatigue or abrasion. Moreover, the wear of balls inside the cage due to boot damage, and inadequate lubrication leads to abrasive wear [5]. There are various methods that help to improve the life of components such as hard-facing, hard-chromium plating, diffusion heat treatment, lubrication films, and surface coatings [6]. The coating technologies include gradient, metastable, multicomponent, and multi-layer coatings [7]. Thin layer coatings have been utilized extensively in various technical applications, including internal combustion engines (ICEs), cutting tools, hard disk drives, automobiles, etc., to increase the wear resistance and performance of mechanical components [8]. Different techniques i.e. physical vapor deposition, thermal spraying, or chemical vapor deposition have produced nano-coatings that have been widely used in recent years to enhance the characteristics and functionality of a wide range of materials [9]. These coatings are also supportive for reducing the wear of friction reducing elements like balls, rollers, cylinders etc. in bearings [10]. These techniques are quite effective in case of ball bearing to protect the balls from wear and improve their life.

The ball performance that is used in rzeppa joint by using multi-body Kinematic model which enables simulation of ball angular
1 velocity [11]. Researchers studied the film thickness of different lubricating greases, oils using optical interferometry on a ball-on-disc setup which are in agreement

International Journal of Engineering Research & Technology (IJERT)
ISSN: 2278-0181
Vol. 14, Issue 09, RTMSE-2026

with base oil film thickness measurements according to Hamrock's equation [12]. The behavior of the Rzeppa joint at distinct parameters by developing different mathematical tools and models was examined and it was concluded that the shape of the contact force is mainly determined from the geometry of the system [13]. The correlation between ball-on-disc and gear test friction measurement was investigated and found to be reasonably good in terms of absolute values [14]. Based on different applications and component designs coating processes are selected. For instance, protecting the surface from oxidation, wear, corrosion, and different tribological issues. Different coating methods are used to increase the life of components and parts. Different coating processes have different coating thicknesses such as Electrochemical (~10-75µm), PVD Sputtering, Evaporation, Ion Implantation, Ion Plating (~1-100µm) etc [15]. The various thermal spray coating processes are applied to structural steels to prevent surface erosion caused by high temperatures or corrosion and erosion combined [16]. In addition to this different physical vapor deposition, chemical vapor deposition, and spray coating methods are used to enhance mechanical and surface properties [17]. The selection criteria of coatings depend upon various factors such as metallurgy of substrate material, availability of required coating material as well as their adaptability to respective coating techniques and accessibility of coating equipment. In addition to this, functional requirements, size, shape, and degradation also contributed to the selection of coating techniques [18]. Nanotechnology focuses on the application of materials having a size of less than 100 nm. Furthermore, nanomaterials have a high surface area to volume ratio, thus can give physical and/or chemical features that are not offered by micro- and macro-sized materials [17]. Nano coatings are composed of crystalline amorphous nano-phase mixtures and have recently increased their value in the field of research and development because of their unique properties against surface protection and tribological issues [19]. A layer of protective coatings formed naturally, synthetically, and deposited over the surface of the material to obtain the required properties. [17]. Moreover, coatings can be divided into two different categories such as metallic and non-metallic coatings [15]. In recent trends, sudden peaks have been observed in the case of physical vapor deposition-based applications. Contemporarily, PVD has vast utilization in actual practice in industries for high-temperature applications. [20]. A nano-coating shows excellent results against wear, corrosion, and oxidation, some of the phases in these coatings provide super-hardness whereas others offer high electrical and or thermal conductivity [21].

TiAlN-coated carbide inserts by PVD method are used for studying the friction and wear mechanisms in the dry sliding condition against steel and cast iron, by using pin-on-disc apparatus under normal load and varied sliding speed [22]. In earlier years, TiAlN coatings were popularly used for wear-resistant properties but nowadays these are used for high-temperature erosion, corrosion, and wear utilizations in different industrial applications [23]. By using a vacuum cathodic arc ion plating method, a layer of TiAlCrN coatings was prepared on substrate alloy and research concluded that these coatings showed superior results against oxidation at a temperature range of 700 to 800ºC whereas, it also reflected improved wear resistance at ambient temperature [24]. TiAlN coatings were deposited by cathodic arc ion plating to study the effect of Al concentration on wear and friction properties and research figured out that with increasing aluminium content in the layer, nano-hardness decreased, and no correlation formed between coefficient of friction and test temperature. At a high temperature of 673K width of the wear track also gets reduced. [25]. Doğuş Özkan et.al studied the different coatings such as TiAlN, AlTiN, and AlCrN with a thickness of ~3.5 µm prepared on the substrate by cathodic arc physical vapor deposition process and they concluded that AlCrN exhibits better wear behaviour than other coatings. [26]. Furthermore, the Sliding tribological performance of AlCrN coating was researched and they revealed that AlCrN undergoes good wear resistant behaviour [27]. Adam Gilewicz et.al tried to probe out the physical configuration and properties of protective coating AlCrN affixed with the help of CAE-PVD technique [28].

MCDM is a kind of numerical tool used by professional decision makers for the material selection problems in which selection is based on multiple criteria's [29]. Eshlaghy & Homayonfar presented are review paper that consists of 628 publications of highly reputed journals in which MCDM is utilized for the purpose of material selection [30]. Ghoushchi et.al used MCDM techniques in transportation systems to predict climatic conditions due to environmental changes [31]. Stojcic et.al reviews the various research publications in which MCDM is utilized to improve the sustainability in the field of engineering [32]. Emovon reviewed various research articles from different platforms for the understanding of various MCDM techniques that are utilized in material selection processes [33]. Rahim presented an enormous number of papers in a single publication to review the different approaches used in MCDM for choosing and supporting material selection methods [34].

2. Experimental & Methodology

2.1 Substrate material

EN-19 has been selected as substrate material being used in steel balls for rzeppa constant velocity joint. EN-19 is medium carbon steel with high hardenability and good fatigue, abrasion and impact resistance. The chemical composition of the substrate is given in Table 1. Spectroscopy analysis was done on Q8 MAGLLAN spark emission spectrometer at the R&D Centre of the bicycle and sewing machine in Ludhiana to confirm the grade and elemental structure of the substrate materials.

Table 1. Chemical Composition (wt %) for EN-19

EN-19	C	S	P	Si	Mn	Cr
Nominal	0.35-0.45	0.050	0.050	0.10-0.35	0.50-0.80	0.90-1.20
Actual	1.010	0.010	0.012	0.250	0.44	1.420

2

International Journal of Engineering Research & Technology (IJERT)
ISSN: 2278-0181
Vol. 14, Issue 09, RTMSE-2026

2.2 Selection and deposition of coatings

In this research work two nano-coatings i.e., Latuma (AlTiN based monolayer) and Alcrona Pro (AlCrN based monolayer) by Oerlikon Balzers, were selected. PVD-DC Magnetron Sputtering method is used for deposition of coatings on EN-19 stainless steel balls being used in Rzeppa joint. The process parameters for LATUMA and ALCRONA PRO as shown in Table 2.

2.3 Characterization of coatings

The surface roughness of the deposited coatings was measured with center line average (CLA) method. The coating thickness values were measured from SEM back scattered micrographs. SEM/EDAX and XRD analysis has been done to know the elemental structure of the coatings. SEM/EDAX analyses were performed at IIT (ICC) Roorkee. Porosity of the as-coated was observed less 0.5 % and measured at Guru Nanak Dev Engineering College Ludhiana.

Table 2. Process parameters for LATUMA and ALCRONA PRO

Parameters	BALINIT-LATUMA	ALCRONA PRO
Layer Type	Mono	Mono
Machine Used	Standard Balzers Rapid Coating System(RCS) Machine	Standard Balzers Rapid Coating System(RCS) Machine
Make	Oerlikon Balzers, Swiss	Oerlikon Balzers, Swiss
Deposition Pressure	3.5 Pa	3.5 Pa
Number of targets	Ti(02), $Ti_{50}Al_{50}$(04)	$Al_{70}Cr_{30}$ (06)
Reactive Gas	Nitrogen	Nitrogen
Coating Thickness	4μm ± 1 μm	4μm ± 1 μm
No. of Target	8	8
Targets Composition	Ti, $Ti_{50}Al_{50}$	$Al_{70}Cr_{30}$
Max Service Temp. (ºC)	1000	1100
Coating Hardness H_{IT}(GPa)	35±3	36±3
Substrate bias voltage	-40V to -170 V	-40V to -170 V
Note: - Target material: Positive biasing. Substrate material: Negative biasing.		

2.4 Wear studies

In this investigation the work has been focused to compare the sliding wear behavior of the nano coated specimens under different environmental conditions, i.e. at room temperature and high temperature (400°C) without lubrication and with lubrication. In first set of experiments the sliding velocity was kept constant i.e. 1m/sec and the normal loads of 30N, 40N and 50N was applied whereas in the second set of experiments normal loads was kept constant and the sliding velocity of 0.5 m/sec, 1 m/sec and 2 m/sec was used. The balls were made to slide against the rotating disc of EN-31 material having hardness of 62-65 HRC. The wear loss and coefficient of friction data was generated with the help of WINDUCOM 2010 software. A ball-on-disc apparatus was used to perform wear testing based on ASTM G-133 standard.

3. Multi Criteria Decision Making (MCDM) techniques

A systematic way to select the best option when several performance criteria are at play is called multi-criteria decision making, or MCDM. It is frequently used in engineering applications where multiple factors, including surface roughness, coating thickness, wear loss, and coefficient of friction, must be considered simultaneously, such as material selection, coating evaluation, and process optimization. It offers an organized approach for ranking several options from best to worst and determining the optimum course of action. MCDM is used in this work to identify the best nano-coating condition, allowing for a thorough evaluation of tribological performance and enhancing the dependability and effectiveness of Rzeppa joint components.

3.1 VIKOR technique

Cavallini et al. [35] used VIKOR-MCDM method to choose the best protective coating out of nine available coatings deposited on Al-7075 alloy. Chauhan and Vaish [36] applied VIKOR and TOPSIS to find out the best soft as well as hard magnetic material. Rai et al. [37] proposed a mathematical MCDM based model in which VIKOR played a vital role in selecting a highly suitable material for a flywheel. Jahan et

International Journal of Engineering Research & Technology (IJERT)
ISSN: 2278-0181
Vol. 14, Issue 09, RTMSE-2026

al. [38] tried to find the foremost material for hip joint prosthesis with the help of the VIKOR-MCDM technique. Giorgetti et al. [39] took the help of C-VIKOR to select an optimal material for a valve seat in an IC engine. The Algorithm of VIKOR-MCDM technique is presented in a flowchart manner given below figure 1:

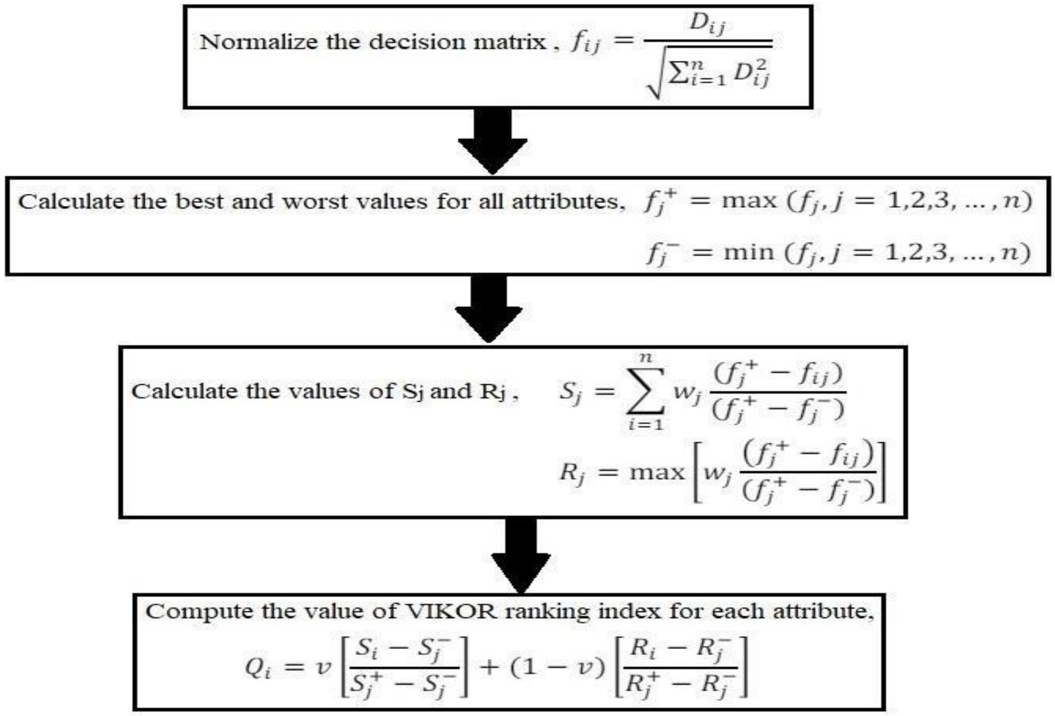

Fig. 1. Flowchart showing the algorithm of VIKOR-MCDM technique [35]

3.2 TOPSIS technique

Tian et al. [40] utilized TOPSIS and grey correlation to select the best green decorative material for interior design. Yadav et al. [41] applied TOPSIS-PSI to select the best composition of hybrid aluminum nanocomposite for marine engineering applications. Chen [42] tried to deduce an MCDM model with the EWM, AHP, and TOPSIS for the selection of building material suppliers. Bhowmik et al. [43] worked on the selection of energy-efficient material with the help of MCDA-EWM-TOPSIS. Dhanalakshmi et al. [44] tried to develop a material selection tool for pyrolysis-based applications with the help of FAHP-TOPSIS-EDAS. The Algorithm of TOPSIS-MCDM technique is presented in a flowchart manner given below figure 2.

International Journal of Engineering Research & Technology (IJERT)
ISSN: 2278-0181
Vol. 14, Issue 09, RTMSE-2026

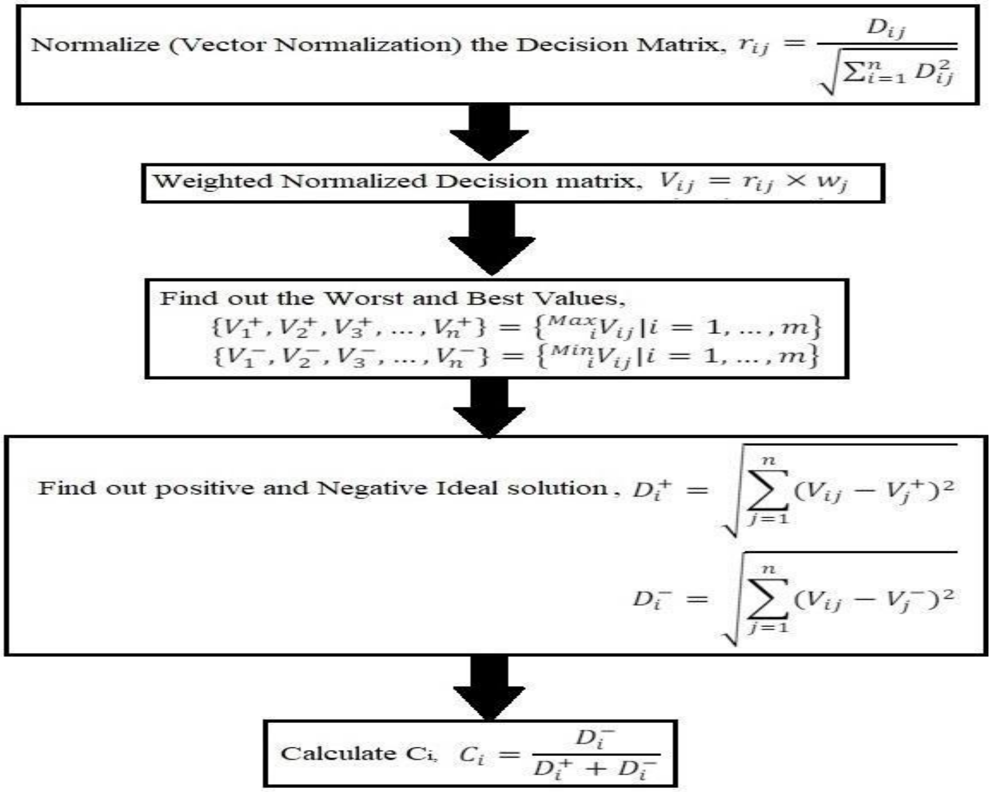

Fig. 2. Flowchart showing the algorithm of TOPSIS-MCDM technique [40]

3.3 EDAS technique

International Journal of Engineering Research & Technology (IJERT)
ISSN: 2278-0181
Vol. 14, Issue 09, RTMSE-2026

Yalcin and Uncu [45] tried to solve the Robert selection problem faced at the industrial level with the help of the EDAS-MCDM technique. Rashid et al. [46] also worked on the robot selection problem by combining three different MCDM techniques TOPSIS-VIKOR-EDAS. Chatterjee et al. [47] worked on gear material selection problem with the help of DoE-EDAS. Nordan and Cengiz [48] applied EDAS for selecting wind turbines and FAHP was used for calculating criteria importance. Kahraman et al. [49] used fuzzy-EDAS for the allocation of solid waste disposal sites. The Algorithm of EDAS-MCDM technique is presented in a flowchart manner given below figure 3.

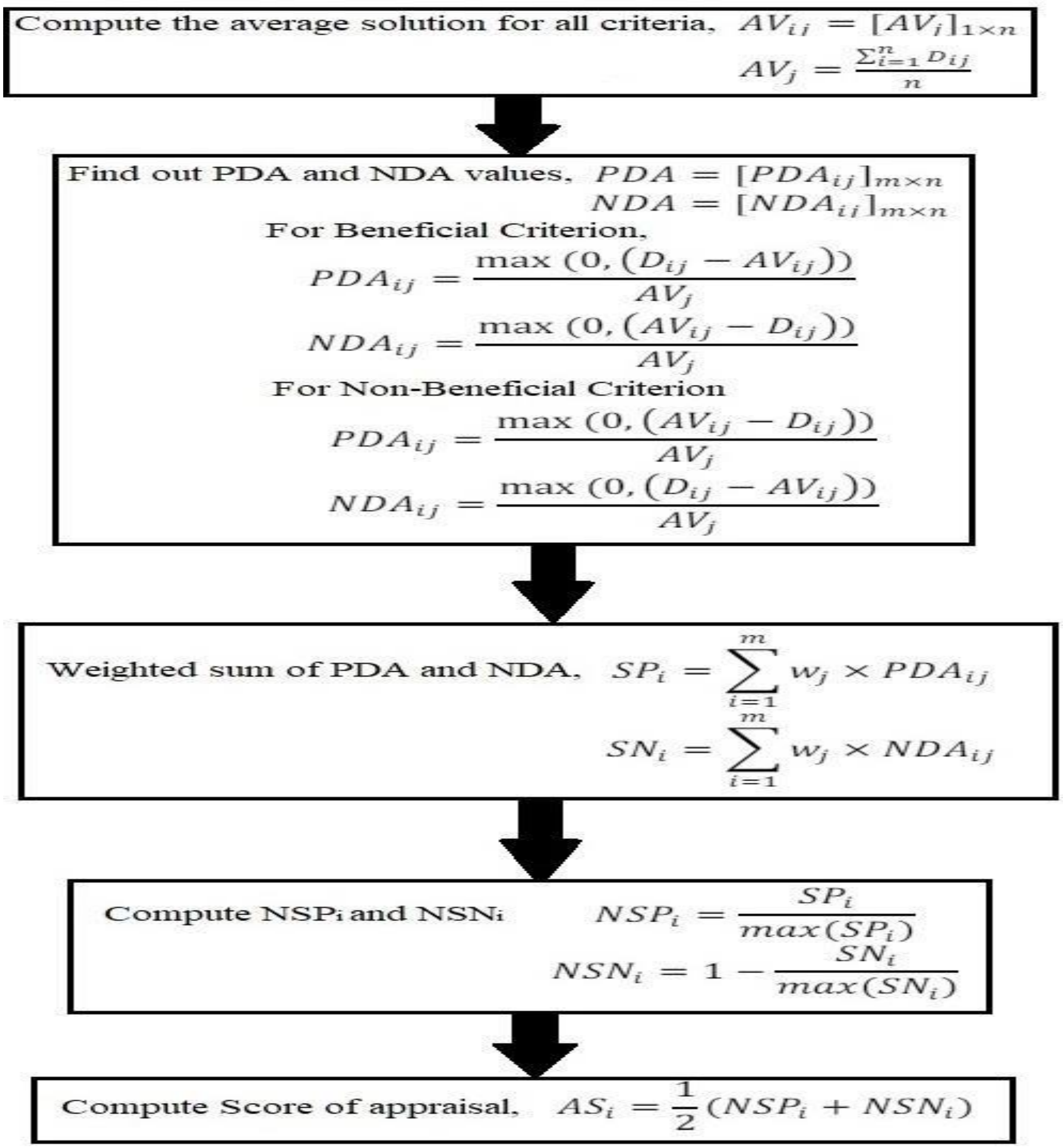

Fig. 3. Flowchart showing the algorithm of EDAS-MCDM technique [45]

3.4 PROMETHEE-II technique

Maity et al. [50] applied PROMETHEE-II to find out the optimal tool steel from the set of ten materials and nine criteria are involved in this study. Vinodh and Girubha [51] used PROMETHEE-II for the implementation of the best sustainable approach in manufacturing industries. Gul et al. [52] used fuzzy-PROMETHEE for the selection of material

International Journal of Engineering Research & Technology (IJERT)
ISSN: 2278-0181
Vol. 14, Issue 09, RTMSE-2026

for the automotive instrument panel. The above-calculated results are validated with the other three fuzzy- MCDM techniques fuzzy-TOPSIS, fuzzy-VIKOR, and fuzzy-ELECTRE. Golam and Afruna [53] utilized FAHP-PROMETHEE for the selection of femoral component material in TKR and sensitivity analysis is also performed. The Algorithm of PROMETHEE-II -MCDM technique is presented in a flowchart manner given below figure 4.

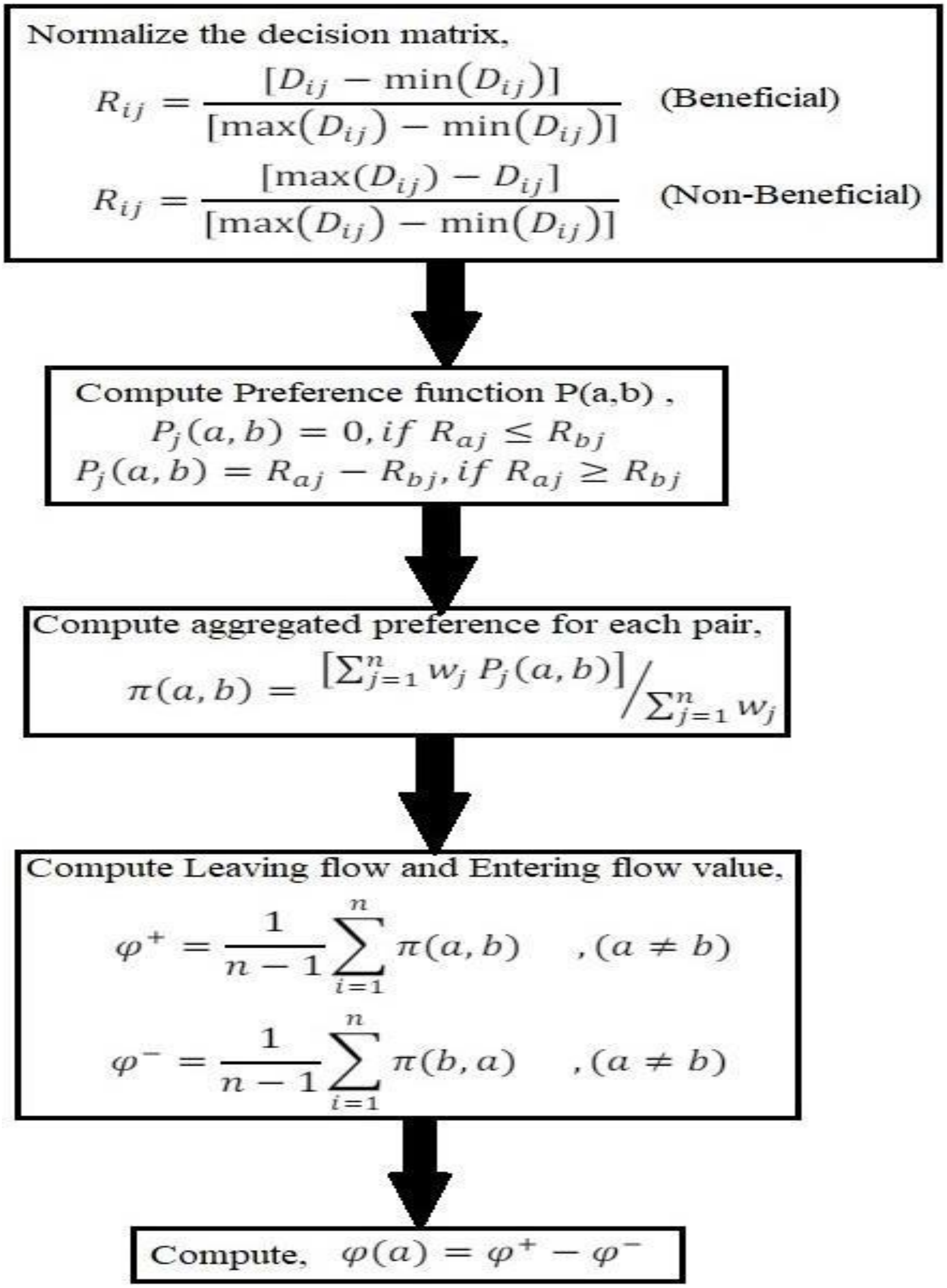

International Journal of Engineering Research & Technology (IJERT)
ISSN: 2278-0181
Vol. 14, Issue 09, RTMSE-2026

Fig. 4. Flowchart showing the algorithm of PROMETHEE-II MCDM technique [50]

Table 3. Results of Surface roughness, coating thickness for various samples

Sr.No.	Coating Condition	Surface Roughness (micron)	Coating Thickness (micron)
1	AlCrN with Lubrication at high temperature	0.08	2.01
2	AlCrN with Lubrication at room temperature	0.08	2.01
3	AlCrN without Lubrication at high temperature	0.08	2.01
4	AlCrN without Lubrication at room temperature	0.08	2.01
5	TiAlN with Lubrication at high temperature	0.027	3.5
6	TiAlN with lubrication at room temperature	0.027	3.5
7	TiAlN without Lubrication at high temperature	0.027	3.5
8	TiAlN without Lubrication at room temperature	0.027	3.5

Table 4. Results of Wear in terms of weight loss and coefficient of friction of worn-out samples

Sr.No.	Coating Condition	Surface Roughness (micron)	oating Thickness (micron)
1	AlCrN with Lubrication at high temperature	0.00382	0.0144
2	AlCrN with Lubrication at room temperature	0.0026	0.0126
3	AlCrN without Lubrication at high temperature	0.0282	0.124
4	AlCrN without Lubrication at room temperature	0.0098	0.1564
5	TiAlN with Lubrication at high temperature	0.0082	0.0126
6	TiAlN with Lubrication at room temperature	0.0042	0.006
7	TiAlN without Lubrication at high temperature	0.03	0.1218
8	TiAlN without Lubrication at room temperature	0.056	0.1308

4. Selection of experimental conditions

The different alternatives and criteria selected in the decision-making matrix for nano-coatings combinations are tabulated in table 5 under different conditions such as: -

Table 5. Notations for different Nano coatings combinations

Notation	Experimental Condition
AlCrN (1)	Coating with lubrication at High Temperature.
AlCrN (2)	Coating with lubrication at Room Temperature.
AlCrN (3)	Coating without lubrication at High Temperature.
AlCrN (4)	Coating without lubrication at Room Temperature.
TiAlN (1)	Coating with lubrication at High Temperature.
TiAlN (2)	Coating with lubrication at Room Temperature.
TiAlN (3)	Coating without lubrication at High Temperature.
TiAlN (4)	Coating without lubrication at Room Temperature.

International Journal of Engineering Research & Technology (IJERT)
ISSN: 2278-0181
Vol. 14, Issue 09, RTMSE-2026

Table 6. Criteria for allocation of Nano coatings

Sr.No.	Notation of criteria	Criteria
1	1_p	Surface Roughness
2	2_p	Coating Thickness
3	3_p	Weight Loss
4	4_p	Coefficient of friction

As mentioned in Table 6 evaluation criteria are selected and are elaborated as follows:

1. Surface Roughness: - It plays an important role in choosing nano-coatings for surface engineering applications. In the case of lubrication, a lower magnitude of surface roughness leads to less wear as well as minimum energy loss while higher values of surface roughness help to keep the lubricants intact and lubrication efficiency [54].
2. Coating Thickness: - The role of coating thickness majorly affects two properties corrosion and wears resistance. A layer of thick coating helps to reduce the corrosion which subsequently increases the life of the substrate and it also helps to decrease the wear and tear of the substrate [55].
3. Wear in terms of weight Loss: -Wear rate plays a vital role while selecting a coating and quantitatively provides coating robustness. It is quite helpful in dropping material degradation [56].
4. Coefficient of friction: - It is quite beneficial in selecting coatings for numerous applications. It helps in finding out wear resistance and increases performance enhancement [57].

Table 7. Decision matrix of Nano-coatings combinations

Condition	Surface Roughness	Coating thickness	Wear in terms of weight Loss	Coefficient of friction
AlCrN (1)	0.08	2.01	0.0038	0.0144
AlCrN (2)	0.08	2.01	0.0026	0.0126
AlCrN (3)	0.08	2.01	0.0282	0.124
AlCrN (4)	0.08	2.01	0.0098	0.1564
TiAlN (1)	0.027	3.5	0.0082	0.0126
TiAlN (2)	0.027	3.5	0.0042	0.006
TiAlN (3)	0.027	3.5	0.03	0.1218
TiAlN (4)	0.027	3.5	0.056	0.1308

Table 7 represents the decision matrix of nano-coatings AlCrN and TiAlN for evaluating the performance under different conditions such as surface roughness, coating thickness, wear in terms of weight loss and coefficient of friction. As indicated in the table AlCrN coatings undergoes better wear resistance as compared to TiAlN coatings.

5. Results and discussion

In this MCDM analysis, while selecting the best optimum coating combination the weightage importance is calculated with the help of the entropy weight method, the calculation of EWM has been shown in the appendix from Tables A1 and A2. After computation, the Weightage for surface roughness, coating thickness, and wear in terms of weight loss and coefficient of friction are 12.40, 3.58, 42.84, and 41.69 respectively. The ranking techniques involved in this work are TOPSIS, VIKOR, EDAS and PROMETHEE-II. For TOPSIS, the computation work is shown in appendix B from Tables B1 and B2. The ranking order for these techniques is: AlCrN (1) > TiAlN (2) > TiAlN (1) > AlCrN (2) > AlCrN (3) > TiAlN (3) > AlCrN (4) > TiAlN (4). For VIKOR, the computation work is shown in appendix C from Tables C1, C2 and C3. The ranking order for these techniques is: TiAlN (2) > TiAlN (1)> AlCrN (2) > AlCrN (1) > AlCrN (4) > TiAlN (3) > AlCrN (3) > TiAlN (4). For EDAS, the computation work is shown in appendix D from Tables D1 to D6. The ranking order for these techniques is: TiAlN (2) > AlCrN (2) > AlCrN (1) > TiAlN (1) > AlCrN (4) > TiAlN (3) > AlCrN (3) > TiAlN (4). For PROMETHEE-II, the computation work is shown in appendix E from Tables E1 to E5. The ranking order for these techniques is: TiAlN (2) > TiAlN (1)> AlCrN (2) > AlCrN (1) > AlCrN (4) > AlCrN (3) TiAlN (3) > TiAlN (4). The comparison of results obtained from all the four ranking techniques are tabulated in Table 8.

Table 8. Comparison of results of all ranking techniques

CONDITION	TOPSIS	VIKOR	EDAS	PROMETHEE-II
AlCrN (1)	1	4	3	4
AlCrN (2)	4	3	2	3
AlCrN (3)	5	7	7	6
AlCrN (4)	7	5	5	5
TiAlN (1)	3	2	4	2
TiAlN (2)	2	1	1	1
TiAlN (3)	6	6	6	7
TiAlN (4)	8	8	8	8

International Journal of Engineering Research & Technology (IJERT)
ISSN: 2278-0181
Vol. 14, Issue 09, RTMSE-2026

6. Conclusions

The ball bearings are used in various industrial and automobile applications. The Balls used in rzeppa joints gets deteriorated after their regular usage in automotives. To enhance the life of balls different protective coatings are utilized. In this research work, experimental and MCDM methods are used to figure out which coating gives better results under various conditions. The following are the conclusions: -

1. 1. A nano-coating TiAlN with lubrication at room temperature obtained from VIKOR, EDAS and PROMETHEE-II.
2. 2. It is observed that in all four ranking techniques, the first four best coating combinations are in lubrication conditions.

3. The result of TOPSIS is completely odd as compared to other three techniques.

4. TiAlN coating without lubrication at room temperature is ranked last in all four MCDM techniques.

Acknowledgements

The authors would like to thank Mr. Jitendra Dabral, DGM operations, Oerlikon Balzers Coatings India Pvt. Limited for his kind cooperation and help. We would also like to thank lab technicians and in-charges for their assistance during experimentation of this research work at Guru Nanak Dev engineering college, Ludhiana.

REFERENCES: -

[1] Ma, S., Zhang, X., Yan, K., Zhu, Y. and Hong, J: A study on bearing dynamic features under the condition of multiball–cage collision. *Lubricants*, *10*(1), 9 (2022) https://doi.org/10.3390/lubricants10010009.

[2] Almeida, M., Bastos, F. and Vecchio, S: Fluid–structure interaction analysis in ball bearings subjected to hydrodynamic and mixed lubrication. *Applied Sciences*, *13*(9),5660 (2023) https://doi.org/10.3390/app13095660

[3] Mao, J., Luo, Y. and Liu, J: Dynamics performance and abrasive wear of the automotive drive shaft. Advances in Mechanical Engineering 6, 713824 (2014) https://doi.org/10.1155/2014/713824

[4] Cirelli, M., Giannini, O., Cera, M., De Simoni, F., Valentini, P.P. and Pennestrì, E: The mechanical efficiency of the Rzeppa transmission joint. Mechanism and Machine Theory 164, 104418 (2021) https://doi.org/10.1016/j.mechmachtheory.2021.104418

[5] Philpott, M.L., Welcher, B.P., Pankow, D.R. and Vandenberg, D: A two- phase circular regression algorithm for quantifying wear in CV joint ball race tracks. *Wear 199* (2), 160-168 (1996) https://doi.org/10.1016/0043-1648(95)05854-0

[6] Jafari, A., Dehghani, K., Bahaaddini, K. and Hataie, R.A: Experimental comparison of abrasive and erosive wear characteristics of four wear-resistant steels. *Wear 416*, 14-26 (2018) https://doi.org/10.1016/j.wear.2018.09.010.

[7] Cho, I.S., Amanov, A. and Kim, J.D: The effects of AlCrN coating, surface modification and their combination on the tribological properties of high-speed steel under dry conditions. *Tribology International* 81, 61-72 (2015) https://doi.org/10.1016/j.triboint.2014.08.003

[8] Mo, J.L., Zhu, M.H., Lei, B., Leng, Y.X. and Huang, N: Comparison of tribological behaviours of AlCrN and TiAlN coatings—Deposited by physical vapor deposition. Wear 263(7-12), 1423-1429. (2007) https://doi.org/10.1016/j.wear.2007.01.051

[9] Fox-Rabinovich, G.S., Weatherly, G.C., Dodonov, A.I., Kovalev, A.I., Shuster, L.S., Veldhuis, S.C., Dosbaeva, G.K., Wainstein, D.L. and Migranov, M.S: Nano-crystalline filtered arc deposited (FAD) TiAlN PVD coatings for high-speed machining applications. Surface and Coatings Technology 177, 800-811 (2004) https://doi.org/10.1016/j.surfcoat.2003.05.004

[10] Polcar, T., Parreira, N.M.G. and Novák, R : Friction and wear behaviour of CrN coating at temperatures up to 500 C. Surface and Coatings Technology 201(9-11), 5228-5235 (2007) https://doi.org/10.1016/j.mechmachtheory.2017.09.005

[11] Shinoda, Y., Mori, A., Yamamoto, T. and Nakamura, T : Ball behavior analysis of Rzeppa constant velocity joint (No. 2016-01-1135). SAE Technical Paper. (2016) https://doi.org/10.4271/2016-01-1135

[12] Cousseau, T., Björling, M., Graça, B., Campos, A., Seabra, J. and Larsson, R: Film thickness in a ball-on- disc contact lubricated with greases, bleed oils and base oils. Tribology International 53, 53-60 (2012) https://doi.org/10.1016/j.triboint.2012.04.018

[13] Shin, J.K., Choi, S.R., Ahn, S.J. and Kim, D.W: Contact ratio analysis of the Rzeppa joint based on full- static modeling. *Mechanism and Machine Theory*, *119*, 236-251(2018)

[14] Björling, M., Miettinen, J., Marklund, P., Lehtovaara, A. and Larsson, R: The correlation between gear contact friction and ball on disc friction measurements. Tribology International 83, 114-119 (2015) https://doi.org/10.1016/j.triboint.2014.11.007

[15] Bose, S: Oxidation-and corrosion-resistant coatings. High temperature coatings: 71-154 (2007) https://doi.org/10.1016/B978-075068252-7/50007-X

[16] Wang, B.Q. and Verstak, A : Elevated temperature erosion of HVOF Cr3C2/TiC–NiCrMo cermet coating. Wear 233,342-351(1999) https://doi.org/10.1016/S0043-1648(99)00242-2

[17] Farooq, S.A., Raina, A., Mohan, S., Arvind Singh, R., Jayalakshmi, S. and Irfan UlHaq, M : Nanostructured coatings: Review on processing techniques, corrosion behaviour and tribological performance. Nanomaterials, 12(8), 1323 (2022) https://doi.org/10.3390/nano12081323

[18] Higuera Hidalgo, V., Belzunce Varela, J., Martínez de la Calle, J.and Carriles Menéndez, A : Characterisation of NiCr flame and plasma sprayed coatings for use in high temperature regions of boilers. *Surface Engineering*, *16*(2), 137-142 (2000) https://doi.org/10.1179/026708400101517035

International Journal of Engineering Research & Technology (IJERT)
ISSN: 2278-0181
Vol. 14, Issue 09, RTMSE-2026

[19] Chawla, V., Sidhu, B.S., Puri, D. and Prakash, S : Performance of plasma sprayed nanostructured and conventional coatings. Journal of the Australian Ceramic Society 44(2),56-62(2008)
[20] Bunshah, R.F. and Weissmantel, C. eds : Handbook of hard coatings (Vol. 3, pp. 77-107). Park Ridge, NJ: Noyes Publications (2001).
[21] Erdemir, A : Review of engineered tribological interfaces for improved boundary lubrication. Tribology International *38*(3), 249-256 (2005) https://doi.org/10.1016/j.triboint.2004.08.008
[22] Grzesik, W., Zalisz, Z., Krol, S. and Nieslony, P : Investigations on friction and wear mechanisms of the PVD-TiAlN coated carbide in dry sliding against steels and cast iron. Wear 261(11-12),1191-1200 (2006) https://doi.org/10.1016/j.wear.2006.03.004
[23] Kalss, W., Reiter, A., Derflinger, V., Gey, C. and Endrino, J.L: Modern coatings in high performance cutting applications. International Journal of Refractory Metals and Hard Materials 24(5), 399-404 (2006) https://doi.org/10.1016/j.ijrmhm.2005.11.005
[24] Qiang, R.U., Shejun, H.U., HUANG, N., Lingzhi, Z.H.A.O., Xiuli, Q.I.U. and Xianqi, H.U: Properties of TiAlCrN coatings prepared by vacuum cathodic arc ion plating. Rare Metals 27(3),251-256 (2008) https://doi.org/10.1016/S1001-0521(08)60124-2
[25] Ohnuma, H., Nihira, N., Mitsuo, A., Toyoda, K., Kubota, K. and Aizawa, T : Effect of aluminum concentration on friction and wear properties of titanium aluminum nitride films. Surface and Coatings Technology 177, 623-626 (2004) https://doi.org/10.1016/S0257-8972(03)00936-8
[26] Özkan, D., Erarslan, Y., Sulukan, E., Kara, L., AlperYılmaz, M. and Yağcı, M.B : Tribological behavior of TiAlN, AlTiN, and AlCrN coatings at boundary lubricating condition. Tribology letters 66(4),152 (2018) https://doi.org/10.1007/s11249-018-1111-1
[27] Mo, J.L. and Zhu, M.H : Sliding tribological behavior of AlCrN coating. Tribology International 41(12), 1161-1168 (2008) https://doi.org/10.1016/j.triboint.2008.02.007.
[28] Gilewicz, A., Jedrzejewski, R., Myslinski, P. and Warcholinski, B : Structure, morphology, and mechanical properties of AlCrN coatings deposited by cathodic arc evaporation. Journal of Materials Engineering and Performance 28, 1522-1531 (2019) https://doi.org/10.1007/s11665-019-03934-2
[29] Mardani, A., Jusoh, A., Nor, K., Khalifah, Z., Zakwan, N. and Valipour, A (2015) Multiple criteria decision- making techniques and their applications–a review of the literature from 2000 to 2014. Economic research-Ekonomskaistraživanja 28(1): 516-571. https://doi.org/10.1080/1331677X.2015.1075139
[30] Toloie-Eshlaghy, A. and Homayonfar, M., :. MCDM methodologies and applications: a literature review from 1999 to 2009. Research Journal of International Studies 21, 86-137(2011)
[31] Ghoushchi, S.J., Ab Rahman, M.N., Soltanzadeh, M., Rafique, M.Z., Hernadewita, Marangalo, F.Y. and Ismail, A.R : Assessing sustainable passenger transportation systems to address climate change based on MCDM methods in an uncertain environment. Sustainability 15(4), 3558 (2023) https://doi.org/10.3390/su15043558
[32] Stojčić, M., Zavadskas, E.K., Pamučar, D., Stević, Ž. and Mardani, A : Application of MCDM methods in sustainability engineering: A literature review 2008–2018. Symmetry 11(3), 350 (2019) https://doi.org/10.3390/sym11030350
[33] Emovon, I. and Oghenenyerovwho, O.S : Application of MCDM method in material selection for optimal design: A review. Results in Materials 7, 100115 (2020) https://doi.org/10.1016/j.rinma.2020.100115
[34] Rahim, A.A., Musa, S.N., Ramesh, S. and Lim, M.K (2020) A systematic review on material selection methods. *Proceedings of the Institution of Mechanical Engineers, Part L:* Journal of Materials: Design and Applications 234(7) : 1032-1059. https://doi.org/10.1177/1464420720916765
[35] Cavallini, C., Giorgetti, A., Citti, P., &Nicolaie, F.: Integral aided method for material selection based on quality function deployment and comprehensive VIKOR algorithm. Materials & Design 47,27-34 (2013) https://doi.org/10.1016/j.matdes.2012.12.009
[36] Chauhan, A., &Vaish, R. Magnetic material selection using multiple attribute decision making approach. Materials & Design 36, 1-5 (2012) https://doi.org/10.1016/j.matdes.2011.11.021
[37] Rai, D., Jha, G. K., Chatterjee, P., & Chakraborty, S. : Material selection in manufacturing environment using compromise ranking and regret theory-based compromise ranking methods: A comparative study.Universal Journal of Materials Science 1(2), 69-77 (2013) https://doi.org/10.13189/ujms.2013.010210
[38] Jahan, A., Mustapha, F., Ismail, M. Y., Sapuan, S. M., &Bahraminasab, M.: A comprehensive VIKOR method for material selection. Materials & Design 32(3), 1215-1221(2011) https://doi.org/10.1016/j.matdes.2010.10.015
[39] A. Giorgetti, C. Cavallini, G. Arcidiacono, P. Citti, : A mixed C-VIKOR fuzzy approach for material selection during design phase: a case study in valve seats for high performance engine, Int. J. Appl. Eng. Res. 12 (12) , 3117–3129 (2017)
[40] Tian, G., Zhang, H., Feng, Y., Wang, D., Peng, Y., & Jia, H. : Green decoration materials selection under interior environment characteristics: A grey-correlation based hybrid MCDM method. Renewable and Sustainable Energy Reviews 81, 682-692 (2018) https://doi.org/10.1016/j.rser.2017.08.050
[41] Yadav, S., Pathak, V. K., &Gangwar, S.: A novel hybrid TOPSIS-PSI approach for material selection in marine applications. Sādhanā 44,1-12 (2019) https://doi.org/10.1007/s12046-018-1020-x
[42] Chen, C. H. : A novel multi-criteria decision-making model for building material supplier selection based on entropy-AHP weighted TOPSIS. Entropy 22(2), 259(2020) https://doi.org/10.3390/e22020259
[43] Bhowmik, C., Gangwar, S., Bhowmik, S., & Ray, A. : Optimum selection of energy-efficient material: A MCDM-based distance approach. Soft Computing Applications, 59-79 (2018) https://doi.org/10.1007/978- 981-10-8049-4_3
[44] Dhanalakshmi, C. S., Madhu, P., Karthick, A., Mathew, M., & Vignesh Kumar, R. : A comprehensive MCDM-based approach using TOPSIS and EDAS as an auxiliary tool for pyrolysis material selection and its application. Biomass conversion and

biorefinery, 1-16 (2020) https://doi.org/10.1007/s13399-020-01009- 0

[45] Yalçın, N., &Uncu, N. : Applying EDAS as an applicable MCDM method for industrial robot selection. Sigma Journal of Engineering and Natural Sciences, 37(3), 779-796 (2019)

[46] Rashid, T., Ali, A., & Chu, Y. M.: Hybrid BW-EDAS MCDM methodology for optimal industrial robot selection. Plos one 16(2): e0246738 (2021) https://doi.org/10.1371/journal.pone.0246738

[47] Chatterjee, P., Banerjee, A., Mondal, S., Boral, S., & Chakraborty, S. : Development of a hybrid metamodel for material selection using design of experiments and EDAS method. Engineering Transactions, 66(2), 187- 207 (2018).

[48] Tüysüz, N., &Kahraman, C.: A novel Z-fuzzy AHP&EDAS methodology and its application to wind turbine selection. Informatica, 34(4), 847-880 (2023) https://doi.org/10.15388/23-INFOR515

[49] Kahraman, C., Keshavarz Ghorabaee, M., Zavadskas, E. K., CevikOnar, S., Yazdani, M., &Oztaysi, B.: Intuitionistic fuzzy EDAS method: an application to solid waste disposal site selection. Journal of Environmental Engineering and Landscape Management 25(1), 1-12 (2017) https://doi.org/10.3846/16486897.2017.1281139

[50] Maity, S. R., & Chakraborty, S.: Tool steel material selection using PROMETHEE II method. The International Journal of Advanced Manufacturing Technology, 78, 1537-1547 (2015) https://doi.org/ 10.1007/s00170-014-6760-0

[51] Vinodh, S., &Girubha, R. J.: PROMETHEE based sustainable concept selection. Applied Mathematical Modelling 36(11), 5301-5308 (2012) https://doi.org/10.1016/j.apm.2011.12.030

[52] Gul, M., Celik, E., Gumus, A. T., &Guneri, A. F.: A fuzzy logic based PROMETHEE method for material selection problems. Beni-Suef University Journal of Basic and Applied Sciences 7(1),68-79 (2018) https://doi.org/10.1016/j.bjbas.2017.07.002

[53] Kabir, G., &Lizu, A: Material selection for femoral component of total knee replacement integrating fuzzy AHP with PROMETHEE. Journal of Intelligent & Fuzzy Systems, 30(6), 3481-3493 (2016) https://doi.org/10.3233/IFS-162094

[54] Holmberg, K., Ronkainen, H. and Matthews, A: Tribology of thin coatings. Ceramics International 26(7), 787-795(2000) https://doi.org/10.1016/S0272-8842(00)00015-8

[55] Bolleddu, V., Racherla, V. and Bandyopadhyay, P.P: Comparative study of air plasma sprayed and high velocity oxy-fuel sprayed nanostructured WC-17wt% Co coatings. The International Journal of Advanced Manufacturing Technology 84, 1601-1613(2016)

[56] Dhakal, D.R., Han, Y.U., Lee, B.G., Kim, T.H., Jang, G.B. and Cho, S.Y: Wear Resistance Behavior of Low-, Mid-, and High-Phosphorus Electroless Ni-P Coatings Heat-Treated in the Air Environment. Coatings 14(5), 648(2024) https://doi.org/10.3390/coatings14050648

[57] Kazlauskas, D., Jankauskas, V. and Antonov, M: Investigation of the Corrosion and Tribological Properties of WC-Co Tools Hardened with PVD Coatings in Solid Oak Wood Processing. Coatings 14(5), 569(2024) https://doi.org/10.3390/coatings14050569

[58] Muhammed, M., Javidani, M., Ebrahimi Sadrabadi, T., Heidari, M., Levasseur, T. and Jahazi, M: A Comprehensive Review of Cathodic Arc Evaporation Physical Vapour Deposition (CAE-PVD) Coatings for Enhanced Tribological Performance. Coatings 14(3), 246 (2024) https://doi.org/10.3390/coatings14030246

International Journal of Engineering Research & Technology (IJERT)
ISSN: 2278-0181
Vol. 14, Issue 09, RTMSE-2026

Appendix A

$$r_{ij} = \frac{x_{ij}}{\sum_{i=1}^{m} x_{ij}}$$

$$e_j = -h\sum_{i=1}^{m} r_{ij}\ln(r_{ij}),\ j = 1,2,3,\ldots,n$$

$$here, h = \frac{1}{\ln m}$$

Table 9. Normalization of decision matrix

	1_p	2_p	3_p	4_p
AlCrN(1)	0.186915888	0.091197822	0.026746954	0.02488766
AlCrN(2)	0.186915888	0.091197822	0.018204733	0.021776702
AlCrN(3)	0.186915888	0.091197822	0.197451337	0.214310404
AlCrN(4)	0.186915888	0.091197822	0.068617841	0.270307639
TiAlN (1)	0.063084112	0.158802178	0.057414928	0.021776702
TiAlN (2)	0.063084112	0.158802178	0.029407646	0.010369858
TiAlN (3)	0.063084112	0.158802178	0.210054614	0.210508123
TiAlN (4)	0.063084112	0.158802178	0.392101947	0.22606291

Table10. Entropy Computations

	1_p	2_p	3_p	4_p
AlCrN(1)	-0.313475993	-0.218393637	-0.096859673	-0.091919664
AlCrN(2)	-0.313475993	-0.218393637	-0.072929502	-0.08333758
AlCrN(3)	-0.313475993	-0.218393637	-0.320318022	-0.330108708
AlCrN(4)	-0.313475993	-0.218393637	-0.183841105	-0.353614984
TiAlN (1)	-0.174319465	-0.292211255	-0.16406034	-0.08333758
TiAlN (2)	-0.174319465	-0.292211255	-0.10370608	-0.047378347
TiAlN (3)	-0.174319465	-0.292211255	-0.327766639	-0.328020291
TiAlN (4)	-0.174319465	-0.292211255	-0.367098941	-0.336142426
$\sum_{i=1}^{m} r_{ij}\ln r_{ij}$	-1.95118183	-2.042419568	-1.636580302	-1.65385958
$e_j = -h\sum_{i=1}^{m} r_{ij}\ln r_{ij}$	0.938320116	0.982196194	0.787028762	0.795338338
$d_j = 1 - e_j$	0.061679884	0.017803806	0.212971238	0.204661662
w_j	0.124075287	0.035814145	0.428413058	0.41169751
Weightage in percentage	12.4075287	3.581414521	42.84130581	41.16975097

Appendix B

$$r_{ij} = \frac{D_{ij}}{\sqrt{\sum_{i=1}^{n} D_{ij}^2}}$$

$$V_{ij} = r_{ij} \times w_j$$

International Journal of Engineering Research & Technology (IJERT)
ISSN: 2278-0181
Vol. 14, Issue 09, RTMSE-2026

$$\{V_1^+, V_2^+, V_3^+, \ldots, V_n^+\} = \{\max_i V_{ij} \mid i = 1, \ldots, m\}$$

$$\{V_1^-, V_2^-, V_3^-, \ldots, V_n^-\} = \{\min_i V_{ij} \mid i = 1, \ldots, m\}$$

$$S_j^+ = \sqrt{\sum_{i=1}^{n} (V_{ij} - V_j^+)^2}$$

$$S_j^- = \sqrt{\sum_{i=1}^{n} (V_{ij} - V_j^-)^2}$$

$$C_i = \frac{S_i^-}{S_i^+ + S_i^-}$$

Table 11. Normalization of decision matrix for TOPSIS

	1_p	2_p	3_p	4_p
AlCrN (1)	0.473746139	0.249002775	0.053842819	0.053538731
AlCrN (2)	0.473746139	0.249002775	0.036646945	0.04684639
AlCrN (3)	0.473746139	0.249002775	0.397478404	0.461027965
AlCrN (4)	0.473746139	0.249002775	0.138130793	0.581490111
TiAlN (1)	0.159889322	0.433586921	0.115578827	0.04684639
TiAlN (2)	0.159889322	0.433586921	0.059198911	0.022307805
TiAlN (3)	0.159889322	0.433586921	0.422849366	0.452848437
TiAlN (4)	0.159889322	0.433586921	0.789318816	0.486310144

Table 12. Weighted Normalized decision matrix for TOPSIS

	1_p	2_p	3_p	4_p	S_j^+	S_j^-	C_i	RANK
AlCrN (1)	5.878018824	0.891782153	2.306696683	2.204176242	4.166607	38.28415	0.901848	1
AlCrN (2)	5.878018824	0.891782153	1.570002978	1.928654211	4.023095	6.444455	0.61566	4
AlCrN (3)	5.878018824	0.891782153	17.02849384	18.98040652	24.09078	26.18343	0.520812	5
AlCrN (4)	5.878018824	0.891782153	5.917703534	23.93980307	23.74978	25.3669	0.516462	7
TiAlN (1)	1.983831353	1.552854496	4.951547855	1.928654211	3.590608	5.880857	0.620903	3
TiAlN (2)	1.983831353	1.552854496	2.536158657	0.918406767	1.170672	3.690869	0.759197	2
TiAlN (3)	1.983831353	1.552854496	18.11541898	18.64365738	24.25639	26.11707	0.518469	6
TiAlN (4)	1.983831353	1.552854496	33.81544876	20.02126753	37.485	39.37871	0.512319	8
	Non-beneficial	Non-beneficial	Non-beneficial	Non-beneficial				
V_j^+	1.983831353	0.891782153	1.570002978	0.918406767				

International Journal of Engineering Research & Technology (IJERT)
ISSN: 2278-0181
Vol. 14, Issue 09, RTMSE-2026

V^-	5.878018824	1.552854496	33.81544876	23.93980307

Appendix C

$$f_{ij} = \frac{D_{ij}}{\sqrt{\sum_{i=1}^{n} D_{ij}^2}}$$

$$f^+ = \max_j (f_j, j = 1, 2, 3 \dots, n)$$

$$f^- = \min_j (f_j, j = 1, 2, 3 \dots, n)$$

$$S_j = \sum_{i=1}^{n} w_j \frac{(f_j^+ - f_{ij})}{(f_j^+ - f_j^-)}$$

$$R_j = \max_j \left[w_j \frac{(f_j^+ - f_{ij})}{(f_j^+ - f_j^-)} \right]$$

$$\boldsymbol{Q}_i = v\left[\frac{S_j - S_j^-}{S_j^+ - S_j^-}\right] + (1 - v)\left[\frac{R_j - R_j^-}{R_j^+ - R_j^-}\right]$$

Table 13. Best and Worst Values for all attribute

	1_p	2_p	3_p	4_p
V^+	0.027	2.01	0.0026	0.006
V^-	0.08	3.5	0.056	0.1564
	Non-beneficial	Non-beneficial	Non-beneficial	Non-beneficial

Table 14. Normalization of decision matrix for VIKOR

	1_p	2_p	3_p	4_p
AlCrN (1)	0.473746139	0.249002775	0.053842819	0.053538731
AlCrN (2)	0.473746139	0.249002775	0.036646945	0.04684639
AlCrN (3)	0.473746139	0.249002775	0.397478404	0.461027965
AlCrN (4)	0.473746139	0.249002775	0.138130793	0.581490111
TiAlN (1)	0.159889322	0.433586921	0.115578827	0.04684639
TiAlN (2)	0.159889322	0.433586921	0.059198911	0.022307805
TiAlN (3)	0.159889322	0.433586921	0.422849366	0.452848437
TiAlN (4)	0.159889322	0.433586921	0.789318816	0.486310144

Table 15. Calculation of Ranks from VIKOR

	1_p	2_p	3_p	4_p	Si	Ri	Qi	rank
AlCrN (1)	104.58519	-4.23279264	41.11066083	13.01301686	154.4761	104.5852	0.104728	4
AlCrN (2)	104.58519	-4.23279264	27.31489856	11.18108847	138.8484	104.5852	0.093765	3
AlCrN (3)	104.58519	-4.23279264	316.7997462	124.5571012	541.7093	316.7997	0.557514	7
AlCrN (4)	104.58519	-4.23279264	108.732512	157.5318123	366.6167	157.5318	0.298737	5
TiAlN (1)	31.109963	-3.78911992	90.63970898	11.18108847	129.1416	90.63971	0.075052	2
TiAlN (2)	31.109963	-3.78911992	45.40770154	4.464017696	77.19256	45.4077	0	1
TiAlN (3)	31.109963	-3.78911992	337.1541495	122.3180776	486.7931	337.1541	0.536366	6

TiAlN (4)	31.109963	-3.78911992	631.1621979	131.4777196	789.9608	631.1622	1	8
				Sj-,Rj-	77.19256	45.4077		
Sj+,Rj+					789.9608	631.1622		

Appendix D

$$AV_{ij} = [AV_j]_{1\times n}$$

$$AV_j = \frac{\sum_{i=1}^{n} D_{ij}}{n}$$

$$PDA = [PDA_{ij}]_{m\times n}$$

$$NDA = [NDA_{ij}]_{m\times n}$$

$$PDA_{ij} = \frac{max(0,(D_{ij} - AV_{ij}))}{AV_j}$$ **(For Beneficial Criteria)**

$$NDA_{ij} = \frac{max(0,(AV_{ij} - D_{ij}))}{AV_j}$$ **(For Beneficial Criteria)**

$$PDA_{ij} = \frac{max(0,(AV_{ij} - D_{ij}))}{AV_j}$$ **(For Non-Beneficial Criteria)**

$$NDA_{ij} = \frac{max(0,(D_{ij} - AV_{ij}))}{AV_j}$$ **(For Non-Beneficial Criteria)**

$$SP_i = \sum_{i=1}^{m} w_j \times PDA_{ij}$$

$$SN_i = \sum_{i=1}^{m} w_j \times NDA_{ij}$$

$$NSP_i = \frac{SP_i}{max(SP_i)}$$

$$NSN_i = 1 - \frac{SN_i}{max(SN_i)}$$

$$AS_i = \frac{1}{2}(NSP_i + NSN_i)$$

International Journal of Engineering Research & Technology (IJERT)
ISSN: 2278-0181
Vol. 14, Issue 09, RTMSE-2026

Where, $0 \leq AS_i \leq 1$

Table 16. Decision matrix for EDAS

	1_p	2_p	3_p	4_p
AlCrN (1)	0.08	2.01	0.00382	0.0144
AlCrN (2)	0.08	2.01	0.0026	0.0126
AlCrN (3)	0.08	2.01	0.0282	0.124
AlCrN (4)	0.08	2.01	0.0098	0.1564
TiAlN (1)	0.027	3.5	0.0082	0.0126
TiAlN (2)	0.027	3.5	0.0042	0.006
TiAlN (3)	0.027	3.5	0.03	0.1218
TiAlN (4)	0.027	3.5	0.056	0.1308
Avj.	0.0535	2.755	0.0178525	0.072325
Non-beneficial		Non-beneficial	Non-beneficial	Non-beneficial

Table 17. Positive distance from Average for EDAS

	1_p	2_p	3_p	4_p
AlCrN (1)	0	0.270417423	0.786024366	0.800898721
AlCrN (2)	0	0.270417423	0.854362134	0.825786381
AlCrN (3)	0	0.270417423	0	0
AlCrN (4)	0	0.270417423	0.451057275	0
TiAlN (1)	0.495327103	0	0.540680577	0.825786381
TiAlN (2)	0.495327103	0	0.764738832	0.917041134
TiAlN (3)	0.495327103	0	0	0
TiAlN (4)	0.495327103	0	0	0

Table 18. Weighted Sum of Positive distance from Average for EDAS

	1_p	2_p	3_p	4_p
AlCrN (1)	0	0.968476885	33.67431025	32.97280089
AlCrN (2)	0	0.968476885	36.60198946	33.99741965
AlCrN (3)	0	0.968476885	0	0
AlCrN (4)	0	0.968476885	19.32388265	0
TiAlN (1)	6.145785244	0	23.16346194	33.99741965
TiAlN (2)	6.145785244	0	32.76241017	37.7543551
TiAlN (3)	6.145785244	0	0	0
TiAlN (4)	6.145785244	0	0	0

Table 19. Negative distance from Average for EDAS

	1_p	2_p	3_p	4_p
AlCrN (1)	0.495327103	0	0	0
AlCrN (2)	0.495327103	0	0	0
AlCrN (3)	0.495327103	0	0.579610699	0.714483235
AlCrN (4)	0.495327103	0	0	1.162461113
TiAlN (1)	0	0.270417423	0	0
TiAlN (2)	0	0.270417423	0	0
TiAlN (3)	0	0.270417423	0.680436914	0.684064984
TiAlN (4)	0	0.270417423	2.136815572	0.808503284

Table 20. Weighted Sum of Negative distance from Average for EDAS

	1_p	2_p	3_p	4_p
AlCrN (1)	6.145785244	0	0	0
AlCrN (2)	6.145785244	0	0	0
AlCrN (3)	6.145785244	0	24.8312792	29.41509687
AlCrN (4)	6.145785244	0	0	47.85823453
TiAlN (1)	0	0.968476885	0	0
TiAlN (2)	0	0.968476885	0	0
TiAlN (3)	0	0.968476885	29.1508059	28.16278505

TiAlN (4)	0	0.968476885	91.54396938	33.28587885

Table 21. Calculation of Ranks from EDAS

	SP_i	SN_i	*NSPi*	*NSNi*	AS_i	
AlCrN (1)	67.61558803	6.145785244	0.881989806	0.951145731	0.916567768	
AlCrN (2)	71.567886	6.145785244	0.933544286	0.951145731	0.942345008	2
AlCrN (3)	0.968476885	60.39216131	0.012632985	0.519928733	0.266280859	7
AlCrN (4)	20.29235954	54.00401978	0.264697162	0.570709549	0.417703355	5
TiAlN (1)	63.30666684	0.968476885	0.825783468	0.992301353	0.909042411	4
TiAlN (2)	76.66255052	0.968476885	1	0.992301353	0.996150677	1
TiAlN (3)	6.145785244	58.28206784	0.08016672	0.536702354	0.308434537	
TiAlN (4)	6.145785244	125.7983251	0.08016672	0	0.04008336	8

Appendix E

$$R_{ij} = \frac{[D_{ij} = min(D_{ij})]}{[max(D_{ij}) - min(D_{ij})]}$$ **(For Beneficial Criteria)**

$$R_{ij} = \frac{[max(D_{ij}) - D_{ij}]}{[max(D_{ij}) - min(D_{ij})]}$$ **(For Non-Beneficial Criteria)**

$$P_j(a,b) = 0, if R_{aj} \leq R_{bj}$$

$$P_j(a,b) = R_{aj} - R_{bj}, if R_{aj} \geq R_{bj}$$

$$\pi(a,b) = \frac{\sum_{j=1}^{n} W_j P_j(a,b)}{\sum_{j=1}^{n} W_j}$$

$$\varphi^+ = \frac{1}{n-1} \sum_{i=1} \pi(a,b), (a \neq b)$$

$$\varphi^- = \frac{1}{n-1} \sum_{i=1}^{n} \pi(b,a), \quad b \neq a$$

$$\varphi(a) = \varphi^+ - \varphi^-$$

Table 22. Maximum and Minimum Values for all attributes (PROMETHEE-II)

	1_p	2_p	3_p	4_p
Maximum	0.08	3.5	0.056	0.1564
Minimum	0.027	2.01	0.0026	0.006

Table 23. Normalized Decision Matrix for PROMETHEE-II

	1_p	2_p	3_p	4_p
AlCrN (1)	0	1	0.977153558	0.944148936
AlCrN (2)	0	1	1	0.956117021
AlCrN (3)	0	1	0.520599251	0.215425532
AlCrN (4)	0	1	0.865168539	0
TiAlN (1)	1	0	0.895131086	0.956117021

International Journal of Engineering Research & Technology (IJERT)
ISSN: 2278-0181
Vol. 14, Issue 09, RTMSE-2026

TiAlN (2)	1	0	0.970037453	1
TiAlN (3)	1	0	0.486891386	0.230053191
TiAlN (4)	1	0	0	0.170212766

Table 24. Calculation of preference functions for all pair of combinations

	1_p	2_p	3_p	4_p
AlCrN(1)- AlCrN(2)	0	0	0	0
AlCrN(1)- AlCrN(3)	0	0	19.55938269	30.00136108
AlCrN(1)- AlCrN(4)	0	0	4.797584433	38.87037658
AlCrN(1)- TiAlN (1)	0	3.581414521	3.513949802	0
AlCrN(1)- TiAlN (2)	0	3.581414521	0.304863225	0
AlCrN(1)- TiAlN (3)	0	3.581414521	21.00347165	29.39914397
AlCrN(1)- TiAlN (4)	0	3.581414521	41.8625344	31.86275939
AlCrN(2)- AlCrN(1)	0	0	0.978771406	0.492723083
AlCrN(2)- AlCrN(3)	0	0	20.5381541	30.49408416
AlCrN(2)- AlCrN(4)	0	0	5.776355839	39.36309966
AlCrN(2)- TiAlN (1)	0	3.581414521	4.492721208	0
AlCrN(2)- TiAlN (2)	0	3.581414521	1.283634631	0
AlCrN(2)- TiAlN (3)	0	3.581414521	21.98224306	29.89186706
AlCrN(2)- TiAlN (4)	0	3.581414521	42.84130581	32.35548247
AlCrN(3)- AlCrN(1)	0	0	0	0
AlCrN(3)- AlCrN(2)	0	0	0	0
AlCrN(3)- AlCrN(4)	0	0	0	8.869015501
AlCrN(3)- TiAlN (1)	0	3.581414521	0	0
AlCrN(3)- TiAlN (2)	0	0	0	0
AlCrN(3)- TiAlN (3)	0	0	20.69860842	31.69851836
AlCrN(3)- TiAlN (4)	0	0	20.85906275	2.463615417
AlCrN(4)- AlCrN(1)	0	0	0	0
AlCrN(4)- AlCrN(2)	0	0	0	0
AlCrN(4)- AlCrN(3)	0	0	14.76179826	0
AlCrN(4)- TiAlN (1)	0	3.581414521	0	0
AlCrN(4)- TiAlN (2)	0	3.581414521	0	0
AlCrN(4)- TiAlN (3)	0	3.581414521	16.20588722	0
AlCrN(4)- TiAlN (4)	0	3.581414521	37.06494997	0
TiAlN (1)- AlCrN(1)	12.4075287	0	0	0.492723083
TiAlN (1)- AlCrN(2)	12.4075287	0	0	0
TiAlN (1)- AlCrN(3)	12.4075287	0	16.04543289	30.49408416
TiAlN (1)- AlCrN(4)	12.4075287	0	1.283634631	39.36309966
TiAlN (1)- TiAlN (2)	0	0	0	0
TiAlN (1)- TiAlN (3)	0	0	17.48952185	29.89186706
TiAlN (1)- TiAlN (4)	0	0	38.3485846	32.35548247
TiAlN (2)- AlCrN(1)	12.4075287	0	0	2.299374389
TiAlN (2)- AlCrN(2)	12.4075287	0	0	1.806651306
TiAlN (2)- AlCrN(3)	12.4075287	0	19.25451946	32.30073547
TiAlN (2)- AlCrN(4)	12.4075287	0	4.492721208	41.16975097
TiAlN (2)- TiAlN (1)	0	0	3.209086577	1.806651306
TiAlN (2)- TiAlN (3)	0	0	20.69860842	31.69851836
TiAlN (2)- TiAlN (4)	0	0	41.55767118	34.16213378
TiAlN (3)- AlCrN(1)	12.4075287	0	0	0
TiAlN (3)- AlCrN(2)	12.4075287	0	0	0
TiAlN (3)- AlCrN(3)	12.4075287	0	0	0.602217102
TiAlN (3)- AlCrN(4)	12.4075287	0	0	9.471232603
TiAlN (3)- TiAlN (1)	0	0	0	0
TiAlN (3)- TiAlN (2)	0	0	0	0
TiAlN (3)- TiAlN (4)	0	0	20.85906275	2.463615417
TiAlN (4)- AlCrN(1)	12.4075287	0	0	0
TiAlN (4)- AlCrN(2)	12.4075287	0	0	0
TiAlN (4)- AlCrN(3)	12.4075287	0	0	0
TiAlN (4)- AlCrN(4)	12.4075287	0	0	7.007617186
TiAlN (4)- TiAlN (1)	0	0	0	0
TiAlN (4)- TiAlN (2)	0	0	0	0
TiAlN (4)- TiAlN (3)	0	0	0	0

Table 25. Pair-wise comparison of all pairs

	AlCrN(1)	AlCrN(2)	AlCrN(3)	AlCrN(4)	TiAlN (1)	TiAlN (2)	TiAlN (3)	TiAlN (4)	Average
AlCrN(1)	0	0	49.56074377	43.66796	7.09536	3.88627	53.9840	77.30671	33.6430
AlCrN(2)	1.47149448	0	51.03223826	45.13945	8.07413	4.86504	55.4555	78.7782	34.9737
AlCrN(3)	0	0	0	8.869015	3.58141	0	52.3971	23.32268	12.5957
AlCrN(4)	0	0	14.76179826	0	3.58141	3.58141	19.7873	40.64636	11.7654
TiAlN (1)	12.9002517	12.4075287	58.94704575	53.05426	0	0	47.3813	70.70407	36.4849
TiAlN (2)	14.7069030	14.2141800	63.96278363	58.07000	5.01573	0	52.3971	75.7198	40.5837
TiAlN (3)	12.4075287	12.4075287	13.0097458	21.87876	0	0	0	23.32268	11.8608
TiAlN (4)	12.4075287	12.4075287	12.4075287	19.41514	0	0	0	0	8.09110
Average	7.69910096	7.34810944	37.66884059	35.72780	3.90686	1.76182	40.2003	55.68579	

Table 26. Calculation of ranks from PROMETHEE-II

	φ^{+}	φ-	$\varphi(a)$	Rank
AlCrN (1)	33.64301219	7.699100966	25.94391122	4
AlCrN (2)	34.97372865	7.348109444	27.62561921	3
AlCrN (3)	12.59574785	37.66884059	-25.07309274	6
AlCrN (4)	11.7654705	35.72780044	-23.96232993	5
TiAlN (1)	36.48493503	3.906866711	32.57806832	2
TiAlN (2)	40.58379103	1.761820203	38.82197083	1
TiAlN (3)	11.86089181	40.200357	-28.33946519	7
TiAlN (4)	8.091104569	55.68578628	-47.59468171	8